ISSN 1063-7834, Physics of the Solid State, 2012, Vol. 54, No. 11, pp. 2155–2164. © Pleiades Publishing, Ltd., 2012.
Original Russian Text © D.A. Balaev, A.A. Dubrovskii, S.I. Popkov, D.M. Gokhfeld, S.V. Semenov, K.A. Shaykhutdinov, M.I. Petrov, 2012, published in Fizika Tverdogo Tela, 2012, Vol. 54, No. 11, pp. 2027–2035.

SUPERCONDUCTIVITY

Specific Features in the Hysteretic Behavior of the Magnetoresistance of Granular High-Temperature Superconductors

D. A. Balaev, A. A. Dubrovskii, S. I. Popkov, D. M. Gokhfeld, S. V. Semenov, K. A. Shaykhutdinov, and M. I. Petrov

Kirensky Institute of Physics, Siberian Branch of the Russian Academy of Sciences, Akademgorodok 50–38, Krasnoyarsk, 660036 Russia

e-mail: smp@iph.krasn.ru

Received February 1, 2012

Abstract—The behavior of the hysteresis of the magnetoresistance $R(H)$ of granular high-temperature superconductors has been investigated under the conditions where the resistive response of the subsystem of grain boundaries close to saturation. The hysteretic dependences $R(H)$ have been measured for $Y_{1-x}Pr_xBa_2Cu_3O_7$ samples at $x = 0.11$ and 0.04 with the transition temperatures $T_C \approx 85.5$ and 91.0 K, respectively. The evolution of the field width of the hysteresis $R(H)$ has been examined by varying the measuring current. The limit of the applicability has been established for the concept of the effective field in the intergranular medium, which was previously proposed for the description of the hysteretic behavior of the magnetoresistance $R(H)$ and thermal magnetic prehistory of the granular high-temperature superconductors. In the studied samples, the approximation of the effective field in the intergranular medium is applicable until the magnetoresistance of the subsystem of grain boundaries exceeds $(90 \pm 5)\%$ of the maximum value.

DOI: 10.1134/S1063783412110030

1. INTRODUCTION

To date, extensive experimental data have been accumulated on the behavior of transport properties exhibited by granular high-temperature superconductors (HTSCs) in external magnetic fields. These investigations are of interest both from the viewpoint of materials science and for basic research. The latter is associated with a unique feature of bulk superconducting materials, namely, the coexistence of two superconducting subsystems, i.e., superconducting grains and grain boundaries, which are considered as a Josephson medium [1]. Below, in this article, the subscript J denotes that the quantity characterizes the intergranular Josephson medium, and the subscript G refers to the quantities characterizing the superconducting grains. As follows for the weak superconductivity, the critical current of the subsystem of grain boundaries j_{CJ} is significantly less than the intragranular critical current j_{CG}. Depending on the experimental conditions and the range of variation in the external magnetic field H, superconducting materials can exhibit a wide variety of effects associated with both the combined influence of these subsystems and the dominance of one of them.

Let us briefly review the studies carried out in this field on classical HTSC systems, such as the Y–Ba–Cu–O, La–Ca–Sr–Cu–O, and Bi–Ca–Sr–Cu–O (YBCO, LSCO, and BSCCO, respectively).

The external magnetic field initially penetrates into the intergranular medium in the form of hypervortices or Josephson vortices [1]. The first critical field of the Josephson medium H_{C1J} is of the order of the Earth's magnetic field or weaker. In the range of weak magnetic fields ($H > H_{C1J}$), the current–voltage characteristics do not depend on the mutual orientation of the external magnetic field **H** and the transport current **I** [2]. In this range of magnetic fields in YBCO, the avalanche dynamics of the penetration of a magnetic flux [3] into a Josephson medium has been observed. The aforementioned features can be explained naturally in the theory of the low-field electrodynamics of a Josephson medium [4].

The dependence of the current–voltage characteristic on the mutual orientation of the transport current and the external magnetic field appears in fields of the order of the first critical magnetic field of superconducting grains H_{C1G}. Under the conditions $j \gg j_{CJ}$ (here, j is the density of the transport current), there arises an angular dependence of the magnetoresistance, proportional to $\sin^2\theta$ ($\angle\theta = \mathbf{j}, \mathbf{H}$) [5–9], which is typical of the processes of magnetic flux flow due to the influence of the Lorentz force [10].

At the same time, in the magnetic field range $H > H_{C1G}$, there appears a hysteresis of the magnetoresistance $R(H)$. The mechanism of the hysteresis $R(H)$ has been investigated in a large number of works [11–27].

It has been established that the hysteresis of the magnetoresistance is caused by the influence of magnetic moments of the superconducting grains on the magnetic field in the intergranular medium [23–27].

For the aforementioned range of magnetic fields, the relaxation processes associated with the output (input) of the vortices from the grains (into the grains) manifest themselves in the relaxation behavior of the magnetoresistance at $H = \text{const}$ [13–17, 24, 25, 28–30]. The hysteresis $R(H)$ exists up to the irreversibility field, above which the hysteresis of the magnetization disappears [18, 27].

The influence of the magnetic moments of the superconducting grains on the magnetic field in the intergranular medium also manifests itself in the existence of a local maximum in the dependence $R(H)$ in the vicinity of the magnetic field in which the dependence $M(H)$ exhibits an extremum [26]. This local maximum has been observed in a number of studies [11, 12, 15–18].

In a series of works [20, 21, 31, 32], the authors observed jumps of the magnetoresistance $R(H)$ for polycrystalline YBCO; in this case, the magnetic field, in which there occurs a jump of the magnetoresistance $R(H)$ ($\approx 2 \times 10^2$ Oe at 77.4 K), is almost independent of the transport current and the angle $\angle\theta = \mathbf{j}, \mathbf{H}$. The authors interpreted this effect as the Bragg glass–vortex glass phase transition, although data on the magnetization were not presented.

Finally, in a particular magnetic field H^* ($H^* \gg H_{C1G}$), the dissipation begins to occur in HTSC grains (for optimally doped YBCO, it is a magnetic field $H^* \sim 60$ kOe at $T = 77.4$ K). This manifests itself in a change of the sign of the curvature of the dependence $R(H)$ near the magnetic field H^* [18, 27, 33, 34]. In magnetic fields close to H^* ($H < H^*$), the magnetoresistance of the subsystem of grain boundaries is a slowly varying function of H; i.e., the resistive response of this subsystem is close to saturation. The beginning of the dissipation inside the grains at $H = H^*$ is accompanied by an additional increase in the dependence $R(H)$. This process of destruction of the superconductivity within the grains (a monotonic increase in the anhysteretic dependence $R(H)$) apparently continues to occur until the second critical magnetic field of the superconductor appears.

The above-described behavior of $R(H)$ in the vicinity of the magnetic field H^*, i.e., the clear separation of the dissipation processes in the subsystems of grain boundaries and grains among the classical HTSC compounds, has been observed for YBCO and LSCO [33]. In strongly anisotropic superconductors, such as BSCCO, this specific feature (the change in the sign of the curvature of the dependence $R(H)$ in the vicinity of H^*) can be observed on textured samples at high transport current densities [34].

The transition from the dissipation in the intergranular medium to the dissipation inside the crystallites also manifests itself in a "two-step" character of the resistive transition in the dependence $R(T)$ in a magnetic field, which has actually been observed for high-temperature superconductors based on YBCO [24, 35–37], LSCO [24, 38], and BSCCO in weak magnetic fields [34, 39]. There are two regions of decrease in the resistance: (i) a sharp drop in R and (ii) a smooth transition to the state "$R = 0$." The first region corresponds to the resistive transition in the grains, and the external magnetic field with a sufficiently large strength ($\sim 10^4$ Oe) exerts an influence on this portion of the dependence $R(T)$. The smooth portion of the dependence $R(T)$ corresponds to the dissipation in the grain boundaries and becomes considerably broadened in weak magnetic fields; moreover, in magnetic fields $H < 10^3$ Oe, the thermomagnetic prehistory takes on significance [30, 33]. In this range of magnetic fields, the thermomagnetic prehistory also manifests itself in the influence of the magnetic field "frozen" in the grains on the current–voltage characteristics [40, 41] and the initial behavior of the magnetoresistance [42, 43].

Thus, the effects associated with the hysteretic behavior of the magnetoresistance and with the thermomagnetic prehistory are adequately explained by the influence of the magnetic moments of the grains on the effective field in the intergranular medium. It was shown that a parameter such as the field width of the hysteresis $R(H)$ does not depend on the transport current in HTSCs of classical compositions (composites based on YBCO, as well as granular YBCO, LSCO, and BSCCO) [23, 24, 27] in a sufficiently wide range of transport currents. The estimation of the effective field in the intergranular medium by means of the comparison of the magnetic data and the field width of the hysteresis $R(H)$ has demonstrated that, in intergranular spaces, the magnetic flux is compressed and the effective field can be one order of magnitude greater than the external magnetic field [44].

The dependences $R(H)$ at high transport current densities have usually been measured in a cryogenic fluid (helium, nitrogen) in order to ensure the effective heat dissipation and to minimize the self-heating effects. In this case, the reduced temperature of measurement $t = T/T_C$ is determined by the transition temperature T_C. Therefore, for the YBCO systems ($T_C \approx 92$ K), the measurements at transport current densities have been performed for the maximum value of the reduced temperature t, which does not exceed 0.84. By "increasing" the value of t and decreasing the transition temperature T_C, it is possible to obtain information about the evolution of the hysteresis of the magnetoresistance under the conditions where the resistive response of grain boundaries is close to saturation, which was not done in [23, 24]. This problem was posed in the present work.

In the YBCO system, the transition temperature T_C can be decreased and, correspondingly, the reduced

temperature t can be increased by means of the partial substitution of praseodymium for yttrium. We have investigated the hysteretic dependences $R(H)$ of the $Y_{1-x}Pr_xBa_2Cu_3O_7$ samples with praseodymium concentrations $x = 0.11$ and 0.04 and the transition temperatures $T_C \approx 85.5$ and ≈91.0 K ($t \approx 0.91$ and ≈0.85), respectively, at different current densities (up to j_C).

2. SAMPLES AND EXPERIMENTAL TECHNIQUE

The experiment was carried out with HTSC samples of the yttrium-containing $Y_{1-x}Pr_xBa_2Cu_3O_7$ system from the series studied in our previous work [45]. This series of samples with different praseodymium concentrations x was prepared according to the standard method of solid-phase synthesis and was characterized in the above-cited work. Below, we present the results obtained for the compositions with praseodymium concentrations $x = 0.11$ and 0.04 and the transition temperatures $T_C \approx 85.5$ and ≈ 91.0 K, respectively. In what follows, the samples with $x = 0.11$ and $x = 0.04$ will be designated as (Y,Pr 0.11) and (Y,Pr 0.04), respectively.

The magnetoresistance $R(H) = U(H)/I$ (where U is the voltage drop and I is the transport current) and current–voltage characteristics $U(I)$ were measured using the standard four-point probe method (electrical contacts were clamping and gold-plated). In these measurements, the sample was placed in a liquid-nitrogen medium, which made it possible to avoid the heating effects at a stable transport current to 0.5 A. The samples were ~8 × 2 × 1 mm^3 in size, and the external magnetic field **H** was applied perpendicular to the direction of the transport current. The sample was cooled in a zero external magnetic field (the Earth's magnetic field was not screened).

The magnetic measurements were performed on a sample-vibrating magnetometer [46]. For these measurements, a cylinder with a cross section of ~5.0 × 0.4 mm^2 was cut from same sample that was used to measure the dependences $R(H)$.

The hysteretic dependences of the magnetoresistance $R(H)$ and the magnetization $M(H)$ in magnetic fields up to 1000 Oe were measured using a copper solenoid. The external magnetic field was increased to the maximum value H_{max} and then decreased to zero. In what follows, the symbols ↑ and ↓ will indicate the increase and the decrease in the external magnetic field, respectively. The sweep rate of the magnetic field was ≈0.5 Oe/s and remained unchanged for measurements of the dependences $R(H)$ and $M(H)$. In order to measure the hysteretic dependence of the critical current on the external magnetic field $I_C(H)$, the magnetic field was stabilized at specific points, and the current–voltage characteristic was measured, after which the magnetic field was changed again and remained constant to the next specified value. The critical current I_C was determined according to the criterion $U = 1$ μV/cm.

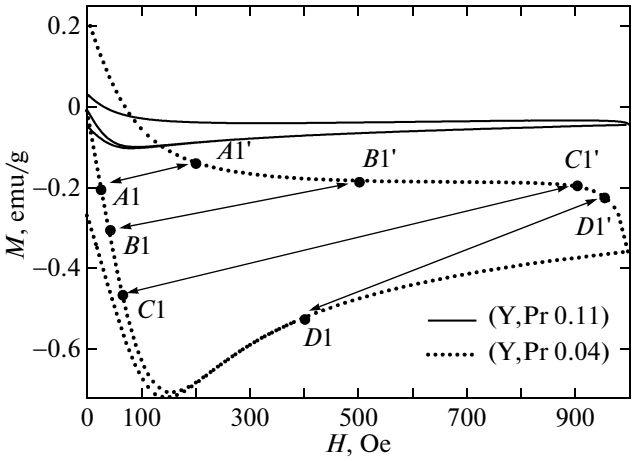

Fig. 1. Hysteretic dependences of the magnetic moment of the (Y,Pr 0.11) and (Y,Pr 0.04) samples at a temperature $T = 77.4$ K. Shown are the forward (from $H_\uparrow = 0$) and reverse (from $H_{max} = 1000$ Oe to $H_\downarrow = 0$) runs of the dependence $M(H)$, which correspond to the path $A1-B1-\ldots-B1'-A1'$, and the fragment of the dependence $M(H)$ with an increase in the magnetic field after cycling ($H_{max} = -1000$ Oe) to the intersection with the initial curve (point $D1$). The specified pairs of points $A1-A1'$, $B1-B1'$, $C1-C1'$, and $D1-D1'$ correspond to the condition $R = \text{const}$ in Fig. 4a.

The hysteretic dependences of the magnetoresistance $R(H)$ in magnetic fields up to 13 kOe were measured using an FL-1 magnet. In measurements of the temperature dependences of the magnetoresistance $R(T)$ in external magnetic fields, the sample was placed in a helium heat-exchange medium. After the measurement of the dependence $R(H)$ at a fixed value of the transport current or the dependence $R(T)$ at a fixed value of the external magnetic field, the sample was heated above T_C and the thermomagnetic prehistory was recorded.

3. RESULTS AND DISCUSSION

3.1. Manifestation of the Contribution from Grain Boundaries and Grains in the Resistive and Magnetic Measurements

The hysteretic dependences of the magnetic moment $M(H)$ measured for the (Y,Pr 0.11) and (Y,Pr 0.04) samples at a temperature $T = 77.4$ K up to the maximum applied magnetic field $H_{max} = 1000$ Oe are shown in Fig. 1. The weaker signal obtained for the (Y,Pr 0.11) sample is associated with the fact that, for the given composition, the measurement temperature corresponds to a higher reduced temperature t. The dependence $M(H)$ is asymmetric with respect to the abscissa axis, which is typical of HTSCs at sufficiently high temperatures and can be caused by the surface

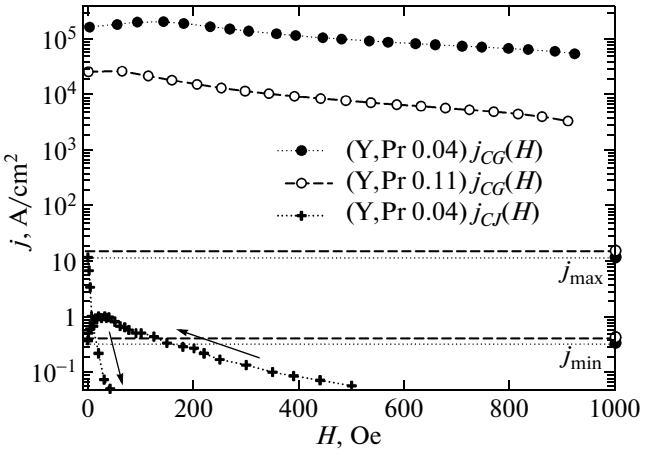

Fig. 2. Field dependences of the intragranular critical current density $j_{CG}(H)$ obtained for the (Y,Pr 0.11) and (Y,Pr 0.04) samples at a temperature $T = 77.4$ K from the dependences $M(H)$ (Fig. 1). The vertical axis Y has a logarithmic scale. The horizontal dashed lines illustrate the range of variation in the density of the transport current in measurements of the dependence $R(H)$. In the same coordinates, the hysteretic dependence of the density of the transport critical current $j_{CJ}(H)$ is shown for the (Y,Pr 0.04) sample (arrows indicate the direction of variation in the external field).

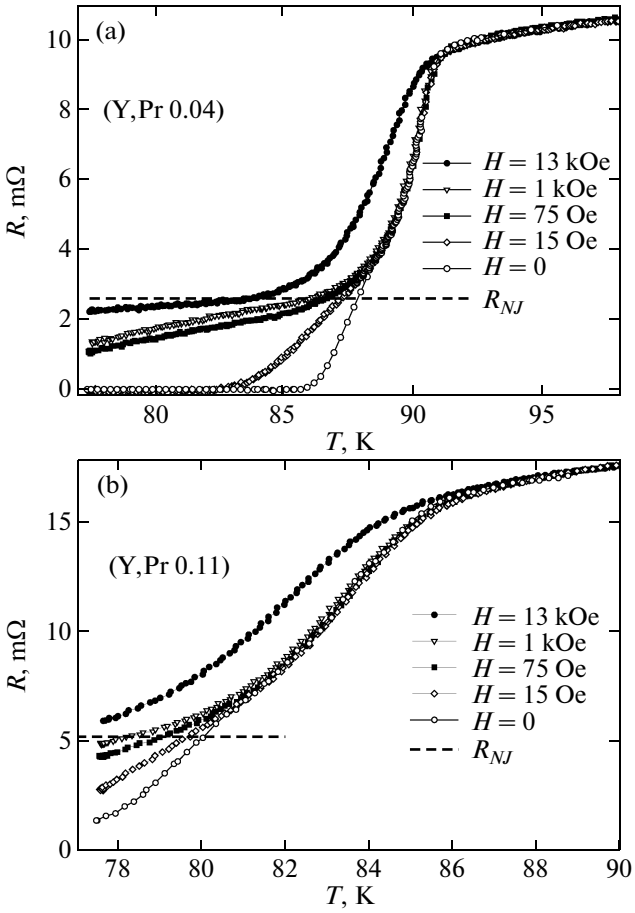

Fig. 3. Resistive transition of the (a) (Y,Pr 0.04) and (b) (Y,Pr 0.11) samples for different values of the external magnetic field. Horizontal lines correspond to the estimates of the "normal" resistance R_{NJ} of the subsystem of grain boundaries (for explanation, see the text).

barriers [47] and depinning [48]. Using the data presented in Fig. 1, we can obtain the field dependence of the intragranular critical current density according to the well-known expression that follows from the Bean model [49]: $j_{CG}(H) = 30\Delta M(H)$ [emu/cm^3]$/d$ [cm] (where ΔM is the "height" of the hysteresis loop of the magnetization in an external magnetic field and d is the average size of the crystallites).

For the value of $d \sim 6$ μm (according to the electron microscopy investigation), we obtained the dependences of the intragranular critical current density on the magnetic field $j_{CG}(H)$ (see Fig. 2). In the same figure, the horizontal dashed lines show the ranges of variation in the transport current density, which were used for measuring the magnetoresistance (see below). It can be seen from this figure that, even for the (Y,Pr 0.11) sample, the transport current j is at least two orders of magnitude smaller than the critical current j_{CG} in a magnetic field of $\sim 10^3$ Oe.

The critical current densities j_C at a temperature $T = 77.4$ K for transport measurements were as follows: $j_C \approx 11.55$ A/cm^2 ($I \approx 340$ mA) for the (Y,Pr 0.04) sample and $j_C \sim 1.3 \times 10^{-2}$ A/cm^2 ($I \approx 0.3$ mA) for the (Y,Pr 0.11) sample. Therefore, in the measurements of the dependences $R(H)$, the ranges of variation in the transport current with respect to the critical current I/I_C were as follows: 0.03–1.03 (10–350 mA) for the (Y,Pr 0.04) sample and $I \gg I_C$ for the (Y,Pr 0.11) sample.

Figure 2 also illustrates the behavior of the hysteretic dependence of the transport critical current density $j_C(H)$ for the (Y,Pr 0.04) sample measured first with an increase in the external magnetic field to $H_{max} = 1000$ Oe and then with a decrease in the external magnetic field H to zero (below the value of $j_C \sim 0.05$ A/cm^2 ($I_C < 1$ mA), the critical current was not measured). Clearly, this value corresponds to the intergranular critical current density $j_{CJ}(H)$.

The dependences $R(T)$ measured for the studied samples in different magnetic fields are shown in Fig. 3. It can be seen from this figure that the resistive transition has a "two-step" character, which is clearly pronounced in the magnetic field. It is natural to interpret the sharp decrease in the magnetoresistance $R(T)$ as a transition in the grains, and the smooth part of the transition (significantly broadened in the external magnetic field), as the response from the grain boundaries. Using the data presented in Fig. 3, we determined the temperatures of the beginning of the superconducting transition $T_C \approx 85.5$ and ≈91.0 K for the (Y,Pr 0.11) and (Y,Pr 0.04) samples, respectively,

which coincided with the beginning of the diamagnetic transition in the dependence $M(T)$.

Let us assume that R_{NJ} is the normal resistance of the grain boundaries, i.e., the resistance in the absence of the influence of superconducting grains on the grain boundaries, for example, at $T = T_C$. At temperatures $T < T_C$, the resistance of the "grains + grain boundaries" system will depend on the current j and the magnetic field H. When the values of the current and the magnetic field are less than the critical parameters of the grains, the resistance of the "grains + grain boundaries" system is less than or equal to R_{NJ}. In our case, the curves of the dependences $R(T)$ (Fig. 3) are used to determine the normal resistance to the grain boundaries R_{NJ}, i.e., the contribution from the grain boundaries to the resistance in the normal state. The spread in the values of the grain boundary length prevents the accurate determination of the resistance R_{NJ}. Furthermore, it is possible that the dependence of the resistance R_{NJ} on the temperature should also be taken into account. The horizontal dashed lines in Fig. 3 represent the estimated contribution from the grain boundaries to the resistance of the sample, which was obtained from the comparison with the data on the dependence $R(H)$ (see below).

3.2. Effective Field in the Intergranular Medium and the Hysteresis R(H)

Figure 4 shows typical dependences $R(H)$ for the (Y,Pr 0.04) sample at transport currents $I = 10$ and 200 mA (Fig. 4a) and for the (Y,Pr 0.11) sample at $I =$ 100 and 200 mA (Fig. 4b).

In an external magnetic field ($H > H_{C1J}$), the HTSC grains have the magnetic moments $\mathbf{M}_G$ ($\mathbf{M} = \Sigma\mathbf{M}_G$); in this case, the lines of the magnetic induction from the magnetic moments $\mathbf{M}_G$ are closed through the grain boundaries (see [23, 25, 27, 44] and figured therein). As a result of the superposition with the external magnetic field $\mathbf{H}$, the magnetic induction in the region of grain boundaries is significantly different from the value of H. If the external magnetic field increases ($H = H_{\downarrow}$, $M < 0$, see Fig. 1; therefore, $M_G < 0$), the lines of the magnetic induction from the magnetic moments of HTSC grains are collinear with the external magnetic field. For the case where the external magnetic field decreases ($H = H_{\downarrow}$), owing to the hysteresis $M(H)$ the contribution from the magnetic moments to the magnetic induction in the intergranular medium becomes smaller. In the field range where the values of M (and M_G) are positive (Fig. 1), the lines of the magnetic induction from the magnetic moments $\mathbf{M}_G$ are directed opposite to the external magnetic field $\mathbf{H}$.

Following [23, 25, 44], we can simplify the complex distribution of the lines of the magnetic induction in the intergranular medium by introducing the effective magnetic field $\mathbf{B}_{\text{eff}}$ in the intergranular medium of the entire sample. In this case, there is a simple empirical relationship between the effective magnetic field, the external magnetic field, and the magnetic moment of the sample:

$$\mathbf{B}_{\text{eff}}(H) = \mathbf{H} - 4\pi\mathbf{M}(H)\alpha. \quad (1)$$

Here, the sign "–" accounts for the direction of the lines of the magnetic induction from the magnetic moments $\mathbf{M}_G$, and the integrated parameter α includes the averaging over the local fields in the grain boundaries, the influence of the demagnetizing factors of the

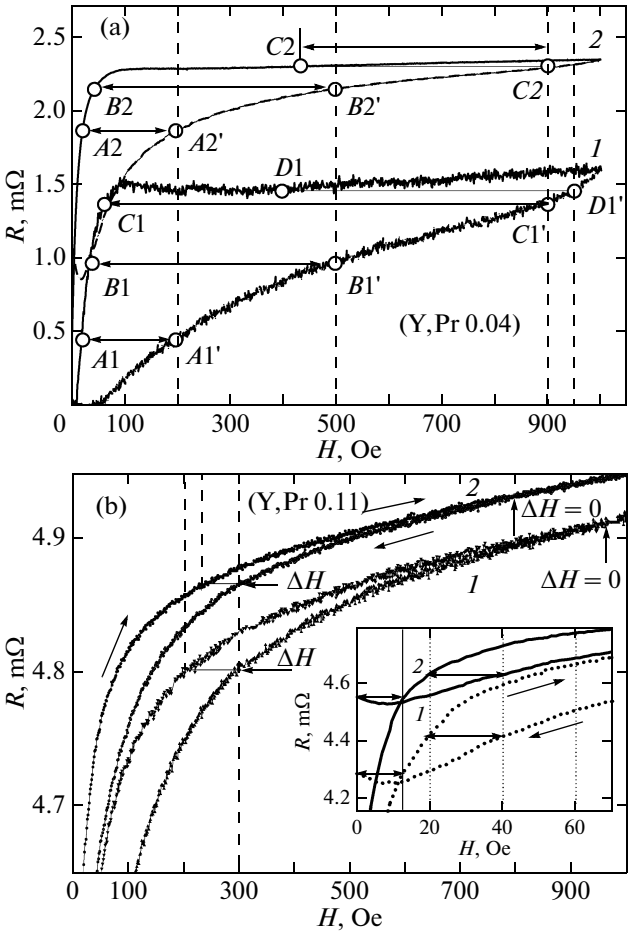

Fig. 4. Selected hysteretic dependences of the magnetoresistance $R(H)$ of the (a) (Y,Pr 0.04) and (b) (Y,Pr 0.11) samples. Horizontal lines (bounded by arrows) illustrate the determination of the field hysteresis width ΔH. $T =$ 77.4 K. (a) $I =$ (*1*) 10 and (*2*) 200 mA. The forward and reverse runs of the dependence $R(H)$ correspond to the path $A1-B1-C1- \ldots -B1'-A1'$. The pairs of points $A1-A1'$, $B1-B1'$, $C1-C1'$, and $D1-D1'$ correspond to the condition $R =$ const, and the magnetic state of the sample for these points is shown in Fig. 1 in similar designations. (b) $I =$ (*1*) 100 and (*2*) 200 mA. Arrows indicate the direction of variation in the external field. The points above which the hysteresis $R(H)$ vanishes ($\Delta H \approx 0$) are denoted. The inset shows in detail the region of weak fields for the (Y,Pr 0.11) sample in the same designations.

grains, and, eventually, determines the degree of compression of the magnetic flux in the intergranular medium [26, 44].

The magnetoresistance caused by the dissipation in the grain boundaries is a monotonic function of the absolute value of this effective field: $R(H) \sim f(|\mathbf{B}_{\text{eff}}(H)|)$. Since there is a hysteresis of the dependence $M(H)$, the dependences $B_{\text{eff}}(H)$ and $R(H)$ also exhibit a hysteresis. On this basis, for two points of the hysteretic dependence $R(H)$ in magnetic fields $H_\uparrow$ and $H_\downarrow$ in which $R(H_\uparrow) = R(H_\downarrow)$, we have $B_{\text{eff}}(H_\uparrow) = B_{\text{eff}}(H_\downarrow)$ and, from expression (1), obtain

$$\Delta H = H_\downarrow - H_\uparrow = 4\pi\alpha(M(H_\uparrow) - M(H_\downarrow)). \quad (2)$$

The parameter ΔH, which is the field width of the hysteresis of the magnetoresistance, is determined by both the parameter α[1] and the values of the magnetic moment at the points $H_\uparrow$ and $H_\downarrow$. The experimental value of the field hysteresis width ΔH in a particular magnetic field $H_\downarrow$ (or $H_\uparrow$) is determined as the length of the horizontal segment that intersects the branches of the hysteretic dependence $R(H)$ at the points with the abscissas $H_\uparrow$ and $H_\downarrow$. Examples of the determination of the parameters ΔH for the (Y,Pr 0.04) sample in magnetic fields $H_\downarrow$ = 200, 500, and 900 Oe ($H_{\max}$ = 1000 Oe) are shown in Fig. 4a: they correspond to the lengths of the segments $A1-A1'$, $B1-B1'$, $C1-C1'$, and $D1-D1'$, respectively. Figure 1 illustrates the arrangement of these points on the branches of the hysteretic dependence $M(H)$ (the thermomagnetic prehistories for the data presented in Figs. 1 and 4a are identical); i.e., at the corresponding points $A1$ and $A1'$, $B1$ and $B1'$, $C1$ and $C1'$, $D1$ and $D1'$ the conditions $R(H_\uparrow) = R(H_\downarrow)$ and $B_{\text{eff}}(H_\uparrow) = B_{\text{eff}}(H_\downarrow)$ are satisfied.

3.3. Field Width of the Hysteresis of the Magnetoresistance. Dependence on the Transport Current and Influence of the Distribution of Grain Boundaries

In our previous works [23, 24], we showed that, for the dependences $R(H)$ measured at different values of the transport current I, the field hysteresis width ΔH remains constant; i.e., it is determined by the values of $M(H_\uparrow)$ and $M(H_\downarrow)$. Indeed, as is shown in Fig. 2, the transport current, which is usually used in the experiments, is considerably less than the intragranular critical current, which determines the value of the magnetic moment. Consequently, it is unlikely that the transport current will affect the magnetic state of the grains. The independence of the field hysteresis width ΔH from the transport current I is illustrated in Fig. 4a for magnetic fields $H_\downarrow$ = 200 Oe and $H_\downarrow$ = 500 Oe. For the dependences $R(H)$ measured at transport currents I = 10 and 200 mA, the lengths of the segments $A1-A1'$ and $A2-A2'$, as well as $B1-B1'$ and $B2-B2'$, are equal to each other, respectively. On the other hand, it can be seen that, at $H_\downarrow$ = 900 Oe, this condition is not satisfied: the segment $C1-C1'$ is larger than the segment $C2-C2'$. For the (Y,Pr 0.11) sample, the decrease in the field hysteresis width ΔH is more pronounced. An example is shown in Fig. 4b for the magnetic field $H_\downarrow$ = 300 Oe (I = 100 and 200 mA). In this case, we can argue that, beginning with a particular value of the magnetic field, the parameter ΔH becomes equal to zero; i.e., the hysteresis disappears. At the same time, in weak magnetic fields, the field hysteresis width ΔH remains unchanged, which illustrates the inset to Fig. 4b for magnetic fields $H_\downarrow$ = 40 Oe and $H_\downarrow$ = 0.

The values of the field hysteresis width ΔH for different values of $H_\downarrow$, which were obtained from measurements of the dependences $R(H)$ of the (Y,Pr 0.11) and (Y,Pr 0.04) samples at transport currents I = 10, 50, 100, 200, and 350 mA for $H_{\max}$ = 1000 and 220 Oe, are shown in Figs. 5a and 5b, respectively.

The data obtained for the (Y,Pr 0.04) sample ($H_{\max}$ = 1000 Oe) (Fig. 5a) indicate that, in the range of relatively weak magnetic fields, the field hysteresis width $\Delta H(H_\downarrow)$ is independent of the transport current. The discrepancy is observed at transport currents I = 350 and 200 mA, and in the range of strong magnetic fields (~800 Oe), it becomes significant. Within the error of the determination of the field hysteresis width ΔH, we can specify the magnetic fields ($H_\downarrow \approx$ 500 Oe (for I = 350 mA) and $H_\downarrow \approx$ 650 Oe (I = 200 mA)) in which this discrepancy appears. For $H_{\max}$ = 220 Oe, there is also a small difference in the values of the transport currents I = 350 and 200 mA in the vicinity of the magnetic field $H_\uparrow \approx$ 200 Oe (Fig. 5b).

The condition $R(H_\downarrow) = R(H_\uparrow)$, which determines the parameter ΔH, also relates to the hysteretic dependence $j_{CJ}(H)$ shown in Fig. 2. Indeed, under the condition $j_{CJ}(H_\downarrow) = j_{CJ}(H_\uparrow)$, the "resistances" in the magnetic fields $H_\downarrow$ and $H_\uparrow$ are also equal to each other, because $R = U/I$, where $U = 1$ μV at $I = I_C$. The behavior of the hysteretic dependence $j_{CJ}(H)$ is a "mirror image" of the behavior of the hysteretic dependences $R(H)$, because, at $I > I_C$, the state with a larger value of R corresponds to a lower value of the critical current, i.e., $R \sim 1/I_C$. Therefore, from the hysteretic dependence $j_{CJ}(H)$ of the (Y,Pr 0.04) sample (Fig. 2), we can also determine the field hysteresis width ΔH as a function of the magnetic field $H_\downarrow$. These values are presented in Fig. 5a. It can be seen from this figure that, in the entire range, where we can obtain the dependences $\Delta H(H_\downarrow)$ according to the condition $j_{CJ}(H_\downarrow) = j_{CJ}(H_\uparrow)$, these values coincide with those determined from the dependence $R(H)$.

The parameter ΔH obtained from the hysteretic dependences $R(H)$ for the (Y,Pr 0.11) sample depends

[1] In this case, the field-independent parameter α is taken as a first approximation. The further reasoning is also valid in the analysis of the functional dependence $\alpha(H)$.

on the current already in a wide range of magnetic fields. For $H_{max} = 1000$ Oe and transport currents $I =$ 350, 200, and 100 mA, there is a range of magnetic fields in which $\Delta H \approx 0$, and it begins with $H_{\downarrow} \approx 750$, 800, and 950 Oe, respectively. Despite the scatter in the data due to the narrowness of the hysteresis $R(H)$, we can note the following specific features. For the maximum current ($I = 350$ mA), the parameter ΔH is always less than the values corresponding to the transport currents $I = 10$–200 mA. This is illustrated in the insets to Figs. 5a and 5b. Within the limits of the error of the determination, the parameter ΔH for transport currents $I = 10$–200 mA in the range of weak magnetic fields does not depend on the current. For $H_{max} =$ 1000 Oe, the divergence in the dependences $\Delta H(H_{\downarrow})$ becomes distinguishable in the vicinity of the magnetic fields $H_{\downarrow} \approx 50$ Oe (see inset to Fig. 5a) for $I =$ 200 mA, $H_{\downarrow} \approx 250$ Oe for $I = 100$ mA, and $H_{\downarrow} \approx 500$ Oe for $I = 50$ mA. For $H_{max} = 220$ Oe, we can also note these characteristic points, i.e., $H_{\downarrow} \approx 50$ Oe for $I =$ 200 mA and $H_{\downarrow} \approx 100$ Oe for $I = 100$ mA). These characteristic points are indicated in Fig. 5 by arrows; the arrows are marked with the symbol corresponding to the dependences $\Delta H(H_{\downarrow})$.

Thus, even for the (Y,Pr 0.04) sample (with a lower reduced temperature of measurement t), there is a dependence of the field hysteresis width ΔH on the transport current. This does not contradict the results reported in our previous paper [23, 24], because, in the cited works, we used lower values of the transport current density. Indeed, for the transport currents $I = 10$–100 mA, the field hysteresis width ΔH (Fig. 5) for this sample does not depend on I.

In order to elucidate the factors responsible for the decrease in the parameter ΔH at high current densities, it is expedient to compare the magnetoresistance with the maximum resistive response from the subsystem of grain boundaries, i.e., with the parameter R_{NJ} introduced in Subsection 3.1. The values of R_{NJ} can be estimated from the dependences $R(T)$ in external magnetic fields (Fig. 3) and from the dependences $R(H)$ for different values of the current. For the (Y,Pr 0.04) sample, this parameter is well consistent with the behavior of the dependences $R(H)$ at transport currents $I = 10$ and 350 mA in magnetic fields up to 13 kOe. This is demonstrated in Fig. 6a. For the (Y,Pr 0.11) sample, we managed to obtain the values of R_{NJ} from the dependences $R(H)$ in magnetic fields up to 13 kOe (see inset to Fig. 6b). In magnetic fields up to ≈3 kOe, the dependences $R(H)$ show a tendency toward saturation; in magnetic fields $H^* \approx 4$ kOe, the functional dependence $R(H)$ changes. This suggests that, in magnetic fields $H \geq H^*$, the dissipation occurs within the grains and that there is a correspondence between the magnetoresistance $R(H^*)$ and the quantity R_{NJ}.

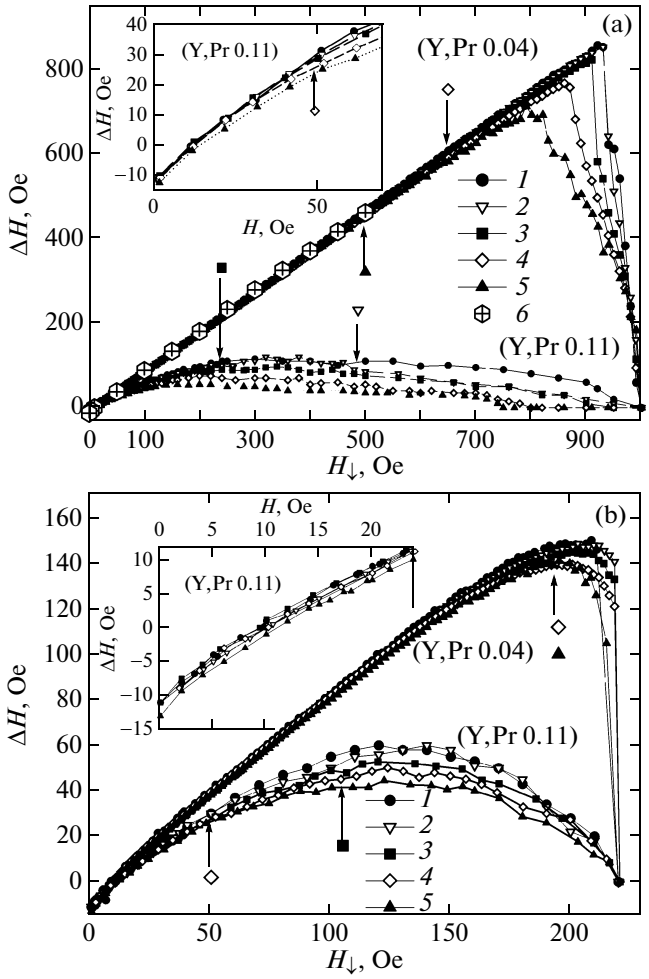

Fig. 5. Field width of the magnetoresistance hysteresis ΔH as a function of $H_{\downarrow}$ obtained from the hysteretic dependence $R(H)$ of the (Y,Pr 0.04) and (Y,Pr 0.11) samples for H_{max} = (a) 1000 and (b) 220 Oe. The insets show the region of weak fields. Numerals specify data obtained for different transport currents I = (*1*) 10, (*2*) 50, (*3*) 100, (*4*) 200, and (*5*) 350 mA. The arrows marked with symbols corresponding to the dependences $R(H)$ indicate magnetic fields in which the parameter ΔH is considered to be decreased within the error of the determination (see the text). Symbols *6* in panel (a) represent data on ΔH obtained from the hysteretic dependence $j_{CJ}(H)$ (Fig. 2) of the (Y,Pr 0.04) sample.

The obtained values of R_{NJ} are compared with the hysteretic dependences $R(H)$ in Figs. 6a and 6b. The dotted lines in these figures correspond to the "saturation" of the resistive response from grain boundaries, and the right vertical axis Y, to the resistance plotted in units of R_{NJ}. It can be seen from Fig. 6b that, for the (Y,Pr 0.11) sample, a variation in the current I within the range 10–350 mA and in the magnetic field up to $H_{max} = 1000$ Oe leads to a change in the resistance R in the range ≈ 0.65–$0.95R_{NJ}$. For the (Y,Pr 0.04) sample, this change corresponds to the range ≈ 0–$0.91R_{NJ}$,

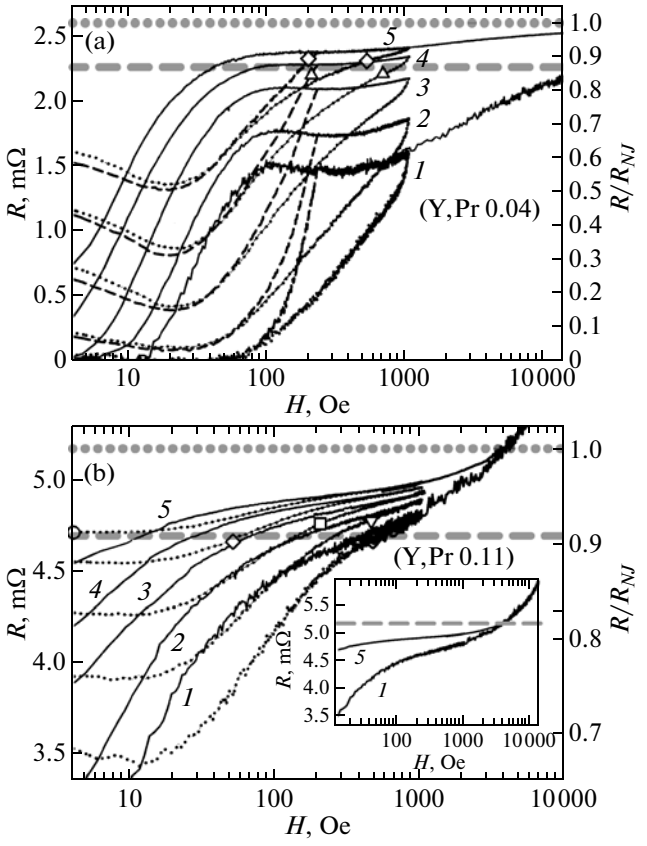

Fig. 6. Hysteretic dependences $R(H)$ of the (a) (Y,Pr 0.04) and (b) (Y,Pr 0.11) samples at a temperature $T = 77.4$ K. The horizontal axis X has a logarithmic scale. Numerals near the curves specify data obtained in measurements of the dependence $R(H)$ for different transport currents $I =$ (*1*) 10, (*2*) 50, (*3*) 100, (*4*) 200, and (*5*) 350 mA. Solid curves show the forward run ($H = H\uparrow$) of the dependence $R(H)$. The reverse run ($H = H_\downarrow$) is shown by the dashed ($H_{max} = 220$ Oe) and dotted ($H_{max} = 1000$ Oe) curves. The horizontal dotted lines indicate the value of R_{NJ} (see the text). The inset in panel (b) shows in detail the dependences $R(H)$ of the (Y,Pr 0.11) sample for $I =$ (*1*) 10 and (*5*) 350 mA. The resistance plotted along the right vertical axis Y is given in units of R_{NJ}. The large symbols corresponding to those identifying the dependences in Fig. 5 specify points at which there appears the dependence of the parameter ΔH on the transport current (as in Fig. 5). The horizontal dashed lines represent the "averaging" of the ordinates of these points.

which is associated with the lower reduced temperature of measurement t.

The symbols in Fig. 6, which identify the dependences $R(H_\downarrow)$, correspond to the magnetic fields $H_\downarrow$ above which there appears a dependence of the field hysteresis width ΔH on the transport current (see Figs. 5a and 5b, where these points are marked by arrows). It can be seen from Fig. 6 that the ordinates of these points have a small spread. The averaging of the values of these ordinates gives the values of $0.88 \pm 0.05R_{NJ}$ and $0.91 \pm 0.03R_{NJ}$ for the (Y,Pr 0.04) and (Y,Pr 0.11) samples, respectively. These averaged values are shown in Fig. 6 by the dashed lines. The values of the magnetic fields, which correspond to the beginning of the dependence of the field hysteresis width ΔH on the transport current (indicated by arrows in Fig. 5), and the values of R_{NJ} were determined from the dependences $R(T)$ (Fig. 3) and $R(H)$ (Fig. 6) with a relative error of 5%.

Thus, we can ascertain that the dependence of the field hysteresis width on the current appears when the magnetoresistance accounts for ~0.9 (± 5–7%) of the maximum resistive response of the subsystem of grain boundaries. In other words, if the experimental point of the dependence $R(H)$ lies on the R axis above the lines $R \sim 0.9R_{NJ}$, there is a dependence of the field hysteresis width ΔH on the current, and vice versa: if the experimental points of the dependence $R(H)$ are located along the R axis below this line, the field hysteresis width ΔH does not depend on the current (including the data obtained for the dependence $j_{CJ}(H)$).

Similar results were obtained for the YBCO sample in which the Pr concentration was intermediate between (Y,Pr 0.11) and (Y,Pr 0.04), namely, $Y_{0.94}Pr_{0.06}Ba_2Cu_3O_7$ ($T_C \approx 88$ K). It turned out that, for this sample, also, the field hysteresis width does not depend on the current for a magnetoresistance smaller than $R \sim 0.9R_{NJ}$.

Let us consider how the closeness of the magnetoresistance to the value of R_{NJ} can affect the parameter ΔH. In the granular sample, of course, there is a distribution of grain boundaries over both their length and the critical current (J_{CJ}). We assume that, for a large value of the transport current and a specific value of the magnetic field H, the magnetoresistance of the junction with the lowest values of the critical current is already close to the resistance R_{NJ} corresponding to these junctions. For the dependence $R(H)$, which is almost at saturation, a change in the magnetic field and, in our case, in the effective magnetic field (see expression (1)) does not lead to a noticeable change in the magnetoresistance; therefore, the hysteresis for this dependence is insignificant. In a stronger magnetic field, the magnetoresistance reaches saturation for junctions with somewhat higher values of j_{CJ} and the hysteresis $R(H)$ is absent even for these junctions. When the Josephson junctions are connected in series with different values of J_{CJ} and a large spread in the values of j_{CJ}, the dependence $R(H)$ for such a chain is the sum of $R(H)$ for individual junctions. In this case, the parameter ΔH will always depend on the current. However, when the Josephson junctions are connected in parallel, the current is redistributed in proportion to their current critical currents [50]. Therefore, if in a random network of Josephson junctions [51, 52], there are junctions with low values of J_{CJ}, their influence has an insignificant effect for $R \ll R_{NJ}$. If the external conditions ($t = T/T_C, j, H$) are such that

R is close to R_{NJ}, the resistance of the junctions with low values of J_{CJ} will be almost equal to the resistance in the normal state. For these junctions, we have $R(H) \approx$ const, and the hysteresis $R(H)$ is absent. The fraction of these junctions increases with an increase in the current or the magnetic field. This will lead to a decrease in the field hysteresis width with an increase in the current and to the disappearance of the hysteresis in the range of magnetic fields considerably below H^* (see Fig. 4b).

It can be expected that, for the granular HTSC with a very narrow distribution function of the grain boundaries over the length, the resistance, at which the dependence of the parameter ΔH on j appears, should be close to R_{NJ}, and vice versa, if the granular HTSC has a broad distribution function, the value of R should decrease.

On this basis, the authors have reason to believe that, for the studied YBCO samples, the influence of the distribution function of the Josephson junctions is identical and manifests itself at a characteristic level of the resistance of the network ~0.9 ($\pm$ 5%)R_{NJ} in the form of the dependence of ΔH on j.

Although in our previous studies [23–25], we used a wide range of transport currents, including the sufficiently low current densities, nonetheless, the magnetoresistance in the measurements of the dependences $R(H)$ did not exceed 80% of the resistance R_{NJ} determined from the dependences $R(T)$.

We note one more experimental fact. For the (Y,Pr 0.04) sample, the curves $R(H_\uparrow)$ (Fig. 6a) at I = 10–100 mA contain a clearly pronounced local maximum in the vicinity of the magnetic field $H_\uparrow \approx 10^2$ Oe. For the (Y,Pr 0.11) sample, the dependence $R(H_\uparrow)$ (Fig. 6b) is a monotonically varying function. This difference can be explained if we estimate the effective field in the intergranular medium according to expression (1). The existence of a local minimum in the dependence $M(H_\uparrow)$ (Fig. 1) manifests itself for the (Y,Pr 0.04) sample in the form of a local maximum in the dependence $B_{\text{eff}}(H)$ and the dependence $R(H_\uparrow)$. For the (Y,Pr 0.11) sample, the magnetic moments at the temperature T = 77.4 K are almost one order of magnitude smaller. Consequently, the contribution from the magnetic moments of the grains, which is proportional to the magnetic moment of the sample, to the effective field will be considerably smaller for the (Y,Pr 0.11) sample. A similar behavior was observed for the BSCCO sample and explained in detail in [26].

4. CONCLUSIONS

In this work, we have investigated the hysteretic dependences of the magnetoresistance $R(H)$ (T = 77.4 K) for different values of the transport current of the granular $Y_{1-x}Pr_xBa_2Cu_3O_7$ (x = 0.04–0.11) superconductor samples. Using the results obtained from these investigations and data on the effect of a magnetic field on the resistive superconducting transition for the studied samples, we have determined the total contribution to the magnetoresistance from the dissipation in the subsystem of grain boundaries, i.e., the resistance of the grain boundaries in the normal state R_{NJ}. The performed analysis of the hysteretic dependence $R(H)$ has revealed that the field width of the hysteresis of the magnetoresistance ΔH is independent of the transport current, provided that the resistance of the subsystem of grain boundaries does not exceed $\approx$ 0.9 ($\pm$ 5%) of the quantity R_{NJ}. Within the error of the determination, this quantity is identical for the studied samples. The independence of the parameter ΔH from the transport current, which was previously demonstrated for granular HTSCs [23–25], follows from the consideration of the granular superconductor as a two-level system ("strong" grains and "weak" Josephson links in grain boundaries). In this work, we have also revealed a decrease in the hysteresis width with an increase in the current for the case where the resistive response of grain boundaries exceeds the characteristic value $\approx$0.9 ($\pm$5%)R_{NJ}, which is explained by the influence of the spread in the values of the grain boundary length and, as a consequence, in the values of the critical current flowing through the intergranular spaces. It can be concluded that, based on a simple relationship for the magnetic moment, the concept of the effective field in the intergranular medium of a granular HTSC consistently describes the main features observed in the hysteretic behavior of the magnetoresistance of granular HTSCs in the specified range of the resistive response of the subsystem of grain boundaries.

ACKNOWLEDGMENTS

This study was supported by the Russian Foundation for Basic Research within the framework of the Regional Competition SIBERIA (project no. 11-02-98007 r-sibir'_a).

REFERENCES

1. E. B. Sonin, JETP Lett. **47** (8), 496 (1988).
2. O. V. Gerashchenko and S. L. Ginzburg, Supercond. Sci. Technol. **13**, 332 (2000).
3. O. V. Gerashchenko, JETP Lett. **86** (7), 470 (2007).
4. S. L. Ginzburg, JETP **79** (2), 334 (1994).
5. D. Lopez and F. de la Cruz, Phys. Rev. B: Condens. Matter **43** (13), 11478 (1991).
6. M. M. Asim and S. K. Hasanin, Solid State Commun. **80** (9), 719 (1991).
7. S. L. Ginzburg, O. V. Gerashenko, and A. I. Sibilev, Supercond. Sci. Technol. **10**, 395 (1997).
8. D. A. Balaev, A. G. Prus, K. A. Shaikhutdinov, and M. I. Petrov, Tech. Phys. Lett. **32** (8), 677 (2006).

9. D. A. Balaev, A. G. Prus, K. A. Shaykhutdinov, D. M. Gokhfeld, and M. I. Petrov, Supercond. Sci. Technol. **20**, 495 (2007).
10. J. Bardeen and M. J. Stephen, Phys. Rev. A **140** (4), A1197 (1965).
11. Y. J. Quian, Z. M. Tang, K. Y. Chen, B. Zhou, J. W. Qui, B. C. Miao, and Y. M. Cai, Phys. Rev. B: Condens. Matter **39** (7), 4701 (1989).
12. S. Shifang, Zh. Yong, Yu Daoqi, Zh. Han, Ch. Zuyao, Q. Yitai, K. Weiyan, and Zh. Qurui, Europhys. Lett. **6** (4), 359 (1988).
13. D. N. Matthews, G. J. Russel, and K. N. R. Taylor, Physica C (Amsterdam) **171**, 301 (1990).
14. I. Felner, E. Galstyan, B. Lorenz, D. Cao, Y. S. Wang, Y. Y. Xue, and C. W. Chu, Phys. Rev. B: Condens. Matter **167**, 134506 (2003).
15. D. Daghero, P. Mazzetti, A. Stepanesku, P. Tura, and A. Masoero, Phys. Rev. B: Condens. Matter **66**, 184514 (2002).
16. N. D. Kuz'michev, JETP Lett. **74** (5), 262 (2001).
17. N. D. Kuz'michev, Phys. Solid State (St. Petersburg) **43** (11), 2012 (2001).
18. C. A. M. dos Santos, M. S. da Luz, and A. J. S. Machado, Physica C (Amsterdam) **391**, 345 (2003).
19. P. Mune, F. C. Fonseca, R. Muccillo, and R. F. Jardim, Physica C (Amsterdam) **390**, 363 (2003).
20. T. V. Sukhareva and V. A. Finkel', Phys. Solid State (St. Petersburg) **50** (6), 1001 (2008).
21. T. V. Sukhareva and V. A. Finkel, JETP **107** (5), 787 (2008).
22. V. V. Derevyanko, T. V. Sukhareva, and V. A. Finkel, Phys. Tech. Phys. **53** (3), 321 (2008).
23. D. A. Balaev, D. M. Gokhfeld, A. A. Dubrovskii, S. I. Popkov, K. A. Shaikhutdinov, and M. I. Petrov, JETP **105** (6), 1174 (2007).
24. D. A. Balaev, A. A. Dubrovskii, K. A. Shaikhutdinov, S. I. Popkov, D. M. Gokhfeld, Yu. S. Gokhfel'd, and M. I. Petrov, JETP **108** (1), 241 (2009).
25. D. A. Balaev, A. A. Dubrovskii, S. I. Popkov, K. A. Shaikhutdinov, and M. I. Petrov, Phys. Solid State (St. Petersburg) **50** (6), 1014 (2008).
26. K. A. Shaikhutdinov, D. A. Balaev, S. I. Popkov, and M. I. Petrov, Phys. Solid State (St. Petersburg) **51** (6), 1105 (2009).
27. D. A. Balaev, S. I. Popkov, S. I. Semenov, A. A. Bykov, K. A. Shaikhutdinov, D. M. Gokhfeld, and M. I. Petrov, Physica C (Amsterdam) **470**, 61 (2010).
28. M. Prester and Z. Marohnic, Phys. Rev. B: Condens. Matter **47**, 2801 (1993).
29. L. Ji, M. S. Rzchowski, N. Anand, and M. Tinkham, Phys. Rev. B: Condens. Matter **47**, 470 (1993).
30. A. V. Mitin, Physica C (Amsterdam) **235–240**, 3311 (1994).
31. V. V. Derevyanko, T. V. Sukhareva, and V. A. Finkel', Phys. Solid State (St. Petersburg) **46** (10), 1798 (2004).
32. V. V. Derevyanko, T. V. Sukhareva, and V. A. Finkel', Phys. Solid State (St. Petersburg) **49** (10), 1829 (2007).
33. D. A. Balaev, A. A. Bykov, S. V. Semenov, S. I. Popkov, A. A. Dubrovskii, K. A. Shaikhutdinov, and M. I. Petrov, Phys. Solid State (St. Petersburg) **53** (5), 922 (2011).
34. D. A. Balaev, S. I. Popkov, S. V. Semenov, A. A. Bykov, E. I. Sabitova, A. A. Dubrovskiy, K. A. Shaikhutdinov, and M. I. Petrov, J. Supercond. Novel Magn. **24**, 2129 (2011).
35. M. A. Dubson, S. T. Herbert, J. J. Calabrese, D. C. Harris, B. R. Patton, and J. Garland, Phys. Rev. Lett. **60** (11), 1061 (1988).
36. C. Gaffney, H. Petersen, and R. Bednar, Phys. Rev. B: Condens. Matter **48** (5), 3388 (1993).
37. H. S. Gamchi, G. J. Russel, and K. N. R. Taylor, Phys. Rev. B: Condens. Matter **50** (17), 12950 (1994).
38. L. Urba, C. Acha, and V. Bekeris, Physica C (Amsterdam) **279**, 92 (1997).
39. A. C. Wright, K. Zhang, and A. Erbil, Phys. Rev. B: Condens. Matter **44** (2), 863 (1991).
40. V. V. Derevyanko, T. V. Sukhareva, and V. A. Finkel', Phys. Solid State (St. Petersburg) **48** (8), 1455 (2006).
41. T. V. Sukhareva and V. A. Finkel, Phys. Solid State (St. Petersburg) **53** (5), 914 (2011).
42. A. A. Sukhanov and V. I. Omel'chenko, Low Temp. Phys. **29** (4), 297 (2003).
43. A. A. Sukhanov and V. I. Omel'chenko, Low Temp. Phys. **30** (6), 452 (2004).
44. D. A. Balaev, S. I. Popkov, E. I. Sabitova, S. V. Semenov, K. A. Shaykhutdinov, A. V. Shabanov, and M. I. Petrov, J. Appl. Phys. **110**, 093918 (2011).
45. M. I. Petrov, Yu. S. Gokhfeld, D. A. Balaev, S. I. Popkov, A. A. Dubrovskiy, D. M. Gokhfeld, and K. A. Shaykhutdinov, Supercond. Sci. Technol. **21**, 085015 (2008).
46. A. D. Balaev, Yu. V. Boyarshinov, M. M. Karpenko, and B. P. Khrustalev, Prib. Tekh. Eksp., No. 3, 167 (1985).
47. Y. Yeshurn, A. P. Malozemoff, and A. Shaulov, Rev. Mod. Phys. **68**, 911 (1993).
48. D. M. Gokhfeld, D. A. Balaev, M. I. Petrov, S. I. Popkov, K. A. Shaykhutdinov, and V. V. Val'kov, J. Appl. Phys. **109**, 033904 (2011).
49. D.-X. Chen, R. W. Gross, and A. Sanchez, Cryogenics **33** (7), 695 (1993).
50. V. V. Schmidt, *The Physics of Superconductors: Introduction to Fundamentals and Applications* (Nauka, Moscow, 1982; Springer, Berlin, 2002).
51. E. Z. Meilikhov, Phys.—Usp. **36** (3), 129 (1993).
52. D. M. Gokhfeld, D. A. Balaev, K. A. Shaykhutdinov, S. I. Popkov, and M. I. Petrov, Physica C (Amsterdam) **467**, 80 (2007).

Translated by O. Borovik-Romanova